High-Temperature-Series Study of Models Displaying Tricritical Behavior. I. Ferromagnetic Planes Coupled Antiferromagnetically*

Fredric Harbus† and H. Eugene Stanley
Physics Department, Massachusetts Institute of Technology, Cambridge, Massachusetts 02139
(Received 16 February 1973)

We introduce two Ising models which exhibit tricritical behavior. Their properties are studied in the presence of a nonzero external magnetic field using the method of high-temperature-series expansions. Both models may simulate some features of metamagnetic materials such as $FeCl_2$ or dysprosium aluminum garnet (DAG). In Paper I we treat the first model, called the "meta" model, which incorporates in-plane ferromagnetic and between-plane antiferromagnetic interactions ($J_{xy} > 0, J_z < 0$). From the two-spin correlation function (expanded to eighth order in inverse temperature), series for the direct and staggered susceptibilities χ and χ_{st} are obtained which are *exact* in the external field. The critical line in the H-T plane is located, and along it χ_{st} appears to diverge with a constant 5/4 exponent $\chi_{st} \sim [T - T_c(H)]^{-5/4}$, consistent with the universality or "smoothness" postulate. Particular attention is focused on behavior near the tricritical point, where the phase transition in the H-T plane changes from second to first order and where the critical-point exponents may be expected to take on a new set of values. At the tricritical point (T_t, H_t), the tricritical susceptibility exponent $\bar{\gamma}$ defined by $\chi \sim (T-T_t)^{-\bar{\gamma}}$ is estimated to be 1/2. The second model is analyzed in Paper II; there we also present the implications of our results for both models in the light of the scaling hypothesis for tricritical points

I. INTRODUCTION

The term "tricritical point" (TCP) was coined by Griffiths,[1] who first discussed its significance as a special symmetry point where a changeover from a second-order to a first-order phase transition occurs. Recently great interest in TCP's has arisen because completely new critical behavior may be expected to characterize such points. More specifically, in the case of metamagnets such as $FeCl_2$,[2] $Ni(NO_3)_2 \cdot 2H_2O$,[3] or dysprosium aluminum garnet (DAG),[4] critical-point exponents at the TCP will in general be different from those along the second-order antiferromagnetic-paramagnetic transition line in the field-temperature (H-T) phase diagram (see Fig. 1). As has been the case before in the field of critical phenomena, this new kind of behavior affords a fruitful arena for active interplay of theory and experiment, and has accordingly come under increasing investigation from many sides. There are now a large number of systems known to display TCP's. In addition to metamagnetic systems, multicomponent mixtures such as He^3-He^4, whose phase diagram is closely analogous to that of metamagnets, have been studied.[5]

It is the purpose of the present work to investigate, by the method of high-temperature series expansions, two Ising models displaying TCP's. The series-expansion approach has in the past been widely applied to obtain detailed predictions for lattice Hamiltonians of magnetic systems.[6] Indeed, in the absence of exact solutions for all but a small class of models (and none for realistic models in three dimensions such as the Ising or

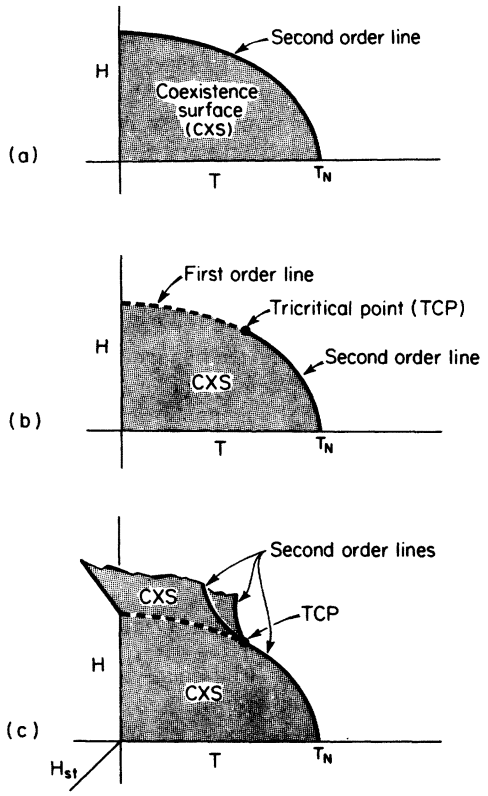

FIG. 1. (a) Schematic phase diagram of "simple" antiferromagnet (nn only isotropic interactions) in the physical H-T field space. (b) Schematic phase diagram of metamagnet in the physical H-T plane. (c) Schematic metamagnetic phase diagram in complete H-T-H_{st} space.

Heisenberg models), much of our knowledge of critical behavior has rested upon results from series analysis. For example, estimates of critical-point exponents from series extrapolations have been extremely instrumental both in the formulation and in the verification of the hypotheses of scaling[7] and universality[8]; these two hypotheses have served to unify much of our current understanding of phase transitions and critical phenomena.

In this paper and in the following paper[9] (hereafter referred to as I and II, respectively) we consider two models displaying tricritical behavior. They are both two-sublattice Ising antiferromagnets with the addition of ferromagnetic interactions within each sublattice. It is the ferromagnetic interactions which are responsible for the tricritical behavior (cf. discussion in Sec. II). These Hamiltonians, for which high-temperature series expansions for nonzero external field have previously not been available, are defined precisely in Sec. II, where we review previous series work on TCP's. Section II also presents a general discussion of the metamagnetic phase diagram, the special features of the TCP, and the predictions of the "smoothness"[10] or universality[8] hypothesis. Section III describes the method of calculation, and may be skipped by the reader not interested in the diagrammatic methods underlying the generation of the high-temperature series.

The analysis of the first model is presented in this paper, while the second model is treated in Paper II. In Sec. IV we present our results for L_1, the second-order critical line in the "physical" $(H\text{-}T)$ plane, showing the calculated phase boundary. We produce evidence germane to the question of the universality of critical exponents along L_1. Section V focuses upon the vicinity of the TCP. We present data allowing an estimate for the *tricritical* susceptibility exponent $\bar{\gamma}$. Throughout, we make comparisons with mean-field-theory (MFT) predictions where appropriate.

II. FEATURES OF PHASE DIAGRAM AND PREVIOUS SERIES-EXPANSION WORK

Landau[11] was the first to discuss a line of phase-transition points changing from second to first order below a certain temperature, and he applied his "classical" theory for critical behavior at this special changeover temperature. However, it was not until much later (1970) that such transition points came to be more fully appreciated, for it was at this time that Griffiths[1] called attention to their significance in the context of current ideas concerning universality or smoothness of critical behavior.

In order to put the Hamiltonians we consider by series in some perspective, we provide in this section a review mainly of the previous *series-expansion* work on TCP and Ising antiferromagnetic critical behavior. Lack of space permits only brief mention of some of the other recent theoretical work. In our discussion, we lean heavily upon the terminology and concepts of Griffiths and Wheeler,[12] whose comprehensive geometric approach to critical phenomena has facilitated the understanding of more complex critical points (e.g., TCP's) and critical surfaces of higher dimensionality, such as occur in multicomponent systems.

Bienenstock[13] and Bienenstock and Lewis[14] applied high-temperature series expansions to the study of the shape of the phase boundary in what will be called a "simple" antiferromagnet. They treat in the presence of an external magnetic field a nearest-neighbor antiferromagnet on loose-packed lattices (i.e., two interpenetrating sublattices), with an exchange constant that is *isotropic* with respect to lattice direction. Their Hamiltonian is therefore written simply as

$$\mathcal{H} = -J \sum_{\langle ij \rangle} s_i s_j - \mu H \sum_i s_i \ . \tag{2.1}$$

Here $J<0$, the sum is over nearest-neighbor pairs only, H is an external field, μ is the magnetic moment per site, and $s_i = \pm 1$. The addition of a staggered magnetic field H_{st} acting *up* on one sublattice A and *down* on the other sublattice B would add a term $-\mu H_{st} \sum_i \eta_i s_i$, where $\eta_i = +1$ for spins on A and -1 on B. Griffiths and Wheeler[12] have emphasized the importance of this third field in understanding the critical behavior of antiferromagnets. The three appropriate field variables are then T, H, and H_{st}, and in this three-dimensional field space the Hamiltonian of Eq. (2.1) has a line of singularities in the $H\text{-}T$ $(H_{st}=0)$ plane [see Fig. 1(a)]. The external field H merely serves to displace the critical temperature $T_c(H)$ at which the second-order phase transition occurs. This transition is associated with critical fluctuations in the order parameter (or ordering "density"), the staggered magnetization, defined as $M_{st} \equiv \frac{1}{2}(M_A - M_B)$. The conjugate field is H_{st}, the "strong-" field direction, and the strongly divergent quantity along the second-order line is the staggered susceptibility $\chi_{st} \equiv (\partial M_{st} / \partial H_{st})$, where the derivative is evaluated for $H_{st} = 0$ and $T \to T_c(H)$.

The other two fields H and T both lie in the plane of the coexistence surface and hence are "weak-" field directions (except at the Néel point T_N, where H is parallel to the critical line and becomes an "independent" direction).[12] The nonordering density M will not undergo strong fluctuations for (2.1), and the direct susceptibility

$$\chi \equiv \left(\frac{\partial M}{\partial H} \right)_{H_{st}=0, T_c(H)}$$

is expected to show only a specific-heat singularity α along the critical line and remain finite at T_N.[10,12,15] The phase transition is thought to remain second order all the way from T_N down to absolute-zero temperature, where of course it must be first order. Although this second-order behavior has not been rigorously proved for this model, it is plausible on the basis of physical and energetic considerations near $T=0$. Further, it is the behavior shown by Fisher's exactly solved superexchange antiferromagnet model.[16]

Griffiths posed a smoothness postulate[10] for critical behavior along lines of critical points such as the line $T_c(H)$ in the simple antiferromagnet. According to this postulate, critical properties will vary smoothly along a second-order line of critical points provided there is no basic change in the underlying first-order phase transition. In particular, critical indices should stay constant along the critical line no matter which point on it is approached.

Rapaport and Domb[17] extended the length of the series used in Ref. 14 for the simple antiferromagnet, and studied several specific predictions of the smoothness postulate. Included is the question of the constancy of the exponent γ_{st} characterizing χ_{st} for various field values. Using Padé-approximant techniques,[18] they verify that for small values of the external field on the simple-cubic and square antiferromagnetic lattices, γ_{st} does not vary from the expected values of 1.25 and 1.75, respectively.

The Hamiltonian (2.1) with $J>0$ (ferromagnetic and in finite field) has been studied by Gaunt and Baker[19] in their study of the $M(H,T)$ function. As will be seen in Sec. III, their finite-field expansions served as an extremely important check on the computer program we employed in our study. Other Ising series in a field have recently been obtained by Ferer and Wortis.[20]

Most real antiferromagnetic materials in fact depart from the ideal behavior of Fig. 1(a) at low temperatures, exhibiting either a spin-flop or metamagnetic transition.[21] The latter is the conceptually simpler of the two, and may be simulated by the Ising models soon to be introduced. A schematic metamagnetic phase diagram in the H-T plane is shown in Fig. 1(b). Figure 1(c) shows the "wings" present in the *complete* H-T-H_{st} space. These are predicted on the basis of mean-field-theory calculations.[1,22] The TCP lies at the intersection of the two critical lines L_2, L_3 bounding each wing and the critical line L_1 in the physical H-T plane. At the TCP, given by $H=H_t$ and $T=T_t$, there is an instability both in the ordering density M_{st} *and* in the nonordering density M.[23] Thus here is an example where the nature of the underlying phase transition does indeed change. This led Griffiths to propose that there may well be a breakdown of smoothness at such a point, and that a new set of critical-point exponents will appear.[1]

The discontinuity in M below T_t is already suggested above T_t by the increasingly steep M vs H isotherms at the critical values of the field $H_c(T)$. The isotherms measured[4] in DAG, the metamagnet on which most data has been obtained thus far, definitely appear to show an infinite slope at T_t. To qualitatively understand this apparently strongly divergent behavior in χ at the TCP in terms of the geometric concepts of Griffiths and Wheeler, we note that because of the wings, H may cease to be a "weak" direction at the TCP. The corresponding quantity at the TCP in He^3-He^4 mixtures also shows strongly divergent behavior.[5(a)]

Although we have been focusing on magnetic systems, the bulk of experimental work on TCP behavior has been on the TCP in He^3-He^4 mixtures. Griffiths proposed[1] a simple scaling theory at the TCP in this system consistent with experimental measurements, and later Blume, Emery, and Griffiths[22] (BEG) introduced a microscopic lattice model for the superfluid and phase-separation transitions. This is a spin-1 Ising Hamiltonian ($s_i=0,\pm1$),

$$\mathcal{H}=-J\sum_{\langle ij\rangle}s_is_j+\Delta\sum_i s_i^2. \tag{2.2}$$

It is solved in the mean-field approximation to yield a TCP and the correct qualitative features, although detailed predictions are not in accord with He-mixture experiments. Series expansions were applied to the BEG model by Saul and Wortis[24] and by Oitmaa,[25] revealing some significant differences with the MFT predictions. No values for TCP exponents are specified, but one may infer an estimate for the tricritical γ from the confluent-singularity form for χ given by Saul and Wortis.

The two tricritical Ising models considered in this work are spin-$\frac{1}{2}$ Ising antiferromagnets with ferromagnetic interactions within each of the two sublattices. We define the first of the tricritical models which we call the "meta" model. The interaction Hamiltonian, defined for the sc lattice, is

$$\mathcal{H}=-J_{xy}\sum_{\langle ij\rangle}^{xy}s_is_j-J_z\sum_{\langle ij\rangle}^{z}s_is_j-\mu H\sum_i s_i. \tag{2.3}$$

Here the interactions are all nearest neighbor (nn), but they have one value J_{xy} for bonds in the x-y plane and another value for bonds connecting spins along the z direction. This is then a model with directional or "lattice" anisotropy. Such models have been studied by series expansions by various authors,[26] *but only in zero field*. We choose $J_{xy}>0$ and $J_z<0$ so that each of the planes is ferromagnetic, but is coupled antiferromagnetically to adjacent planes. This corresponds to the signs of the interactions present in metamagnetic materials

such as $FeCl_2$. In our model, one "sublattice" would consist of all even-numbered planes, and the other "sublattice" of all odd-numbered planes. A staggered field would alternate direction from one plane to the next. A pictorial representation of the ordered state is shown in Fig. 2(a).

The second tricritical model we call the nnn model because it incorporates next-nearest-neighbor (nnn) interactions. The Hamiltonian is the same as (2.1) with the addition of second-neighbor ferromagnetic exchange, so that

$$\mathcal{H} = -J_1 \sum_{\langle ij \rangle}^{\text{nn}} s_i s_j - J_2 \sum_{[ij]}^{\text{nnn}} s_i s_j - \mu H \sum_i s_i . \qquad (2.4)$$

Here $J_1 < 0$, $J_2 > 0$, and the first and second sums are over nn and nnn spins, respectively, again on the sc lattice. In Eq. (2.4) there are two sublattices consisting of two interpenetrating fcc lattices. The ordered antiferromagnetic state in one plane is shown schematically in Fig. 2(b).

The nnn Hamiltonian [Eq. (2.4)] has been previously studied[27] by series techniques, but only for zero field. Although no previous series work exists, Monte Carlo studies for (2.4) in finite field have been carried out quite recently.[28] A tricritical point was located and estimates of certain tricritical exponents were given (the high-temperature susceptibility exponent $\bar{\gamma}$ and the exponent $\bar{\beta}$ describing the discontinuity in magnetization below T_t). The same Monte Carlo techniques have also now[29] been applied to the meta model with exactly the same choice of parameters J_{xy} and J_z discussed by us in subsequent sections, thereby complementing and providing valuable checks on our series work.

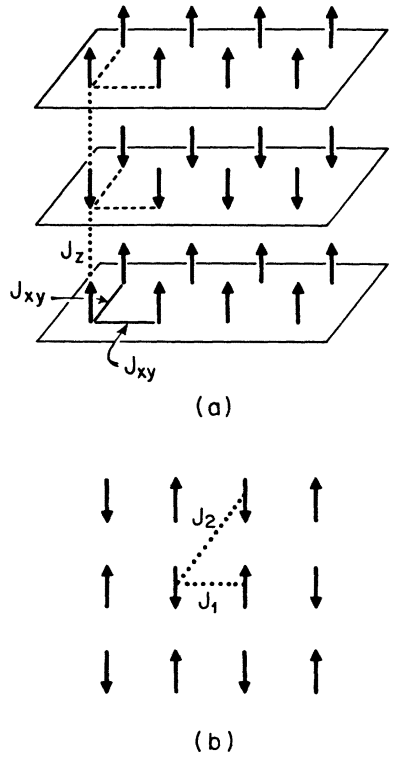

FIG. 2. (a) Schematic diagram of perfectly ordered $T = 0$ state in meta model, showing in-plane ferromagnetic bonds J_{xy} and between-plane antiferromagnetic bonds J_z. (b) One plane of ordered state of nnn model, showing antiferromagnetic nn bonds J_1 and ferromagnetic second-neighbor bonds J_2.

Finally, for a detailed mean-field-theory treatment of two-sublattice Ising antiferromagnets in a magnetic field, the reader is referred to the work of Bidaux *et al.*[30]

We may gain some physical insight into the behavior of the two tricritical models we consider by noting that in either case, the ferromagnetic exchange serves to stabilize the order within a sublattice. At low temperatures, most spins on one sublattice are oriented parallel to an external field, those on the other antiparallel. A big enough external field, the critical field, will flip the spins on the antiparallel sublattice, and the system passes from an antiferromagnetic phase (where the order parameter is nonzero) to the paramagnetic phase (where the order parameter *is* zero). Because spins on this sublattice are locked together due to the J_{xy} or J_2, a finite discontinuity in magnetization results, and the transition is first order [see Fig. 1(b)]. This discontinuity is maximum at $T = 0$, and decreases to zero at the TCP. At higher temperatures, the order within a sublattice is not strong enough to overcome the randomizing thermal effects, and the phase transition is second order up to the Néel point, beyond which it disappears completely.

To conclude this section, we mention briefly some of the other recent theoretical work on TCP's. A more detailed scaling theory at the TCP (than Ref. 1) was developed by Riedel[23] and used to describe He^3-He^4 mixtures. Hankey *et al.*[31] extended the scaling hypothesis to include the third ordering field and discussed the consequences for the shape of the critical lines at the TCP. "Double-power" laws near the TCP have been discussed by Riedel[23,32] and by Chang *et al.*[33] (Such laws and other aspects of TCP scaling will be considered in more detail in Paper II.)

Riedel and Wegner[34] investigated TCP behavior using the Wilson renormalization-group approach,[35] obtaining mean-field-like tricritical exponents for $d = 3$. Recently, logarithmic corrections to tricritical thermodynamic functions have been obtained.[36] Kortman[37] has presented a parametric equation of state near the TCP, and droplet-model descriptions have been examined by Reatto[38] and Stauffer.[39] Finally, several workers[40] have studied one-dimen-

sional Ising chains with competing short- and long-range interactions. These models display tricritical and other hypercritical (e.g., tetracritical) points.

III. GENERATION OF HIGH-TEMPERATURE SERIES

A computer program which implements the renormalized linked-cluster expansion theory of Wortis *et al.*[41] is employed to generate the high-temperature series for the two models we consider. The program calculates the two-spin correlation function $C_2(\vec{r}) \equiv \langle s_0 s_{\vec{r}} \rangle - \langle s_0 \rangle \langle s_{\vec{r}} \rangle$ from the origin to all sites $\vec{r}$ in an appropriate reduced space on the lattice. The calculation is effected by constructing a set of diagrams on the lattice, and evaluating their contribution to successive powers of inverse temperature. In the resulting perturbation expansion for $C_2(\vec{r})$ in $1/k_B T$, the exchange constants J_{xy} and J_z (or J_1 and J_2) are absorbed in the coefficients of the expansion, and if desired may be factored out in the end to give an expansion in a dimensionless variable of an (exchange energy)$/k_B T$.

As in earlier linked-cluster expansions, the summation of diagrams in this program is of the "free" type, so that there is no excluded volume problem and lattice constants are easily evaluated. Englert[42] carried through the one-point or "vertex" renormalization of the Ising-model linked-cluster expansion, and later the Wortis group went further to do the two-point or "bond" renormalization. As the level of sophistication of the theory increases, there is a corresponding decrease in the number of diagrams which must be considered explicitly. Under the various renormalizations, large classes of graphs become topologically equivalent, and only the underlying "skeleton" of a given graph is important. This, of course, occurs at the cost of much increased algebraic complexity, since each skeleton no longer carries its bare value but must include contributions from the entire class of graphs which reduce to it when the extra decorations are cut away.[43]

Using the fact that decorations of a skeletal graph need not be considered separately and that, of those remaining graphs, the more complex ones may be built up using simpler ones already evaluated, one may iterate the basic integral equations of the two-point-renormalization theory. Every higher-order term in $\beta \equiv 1/k_B T$ is evaluated using information from the lower-order terms already available. The *only* diagrams which cannot be evaluated in this manner are the class of so-called "elementary" diagrams, and these must be constructed explicitly in the computer program at the point where they first enter. Their number rapidly proliferates as one goes to higher orders in β, and this is the chief limiting factor in computer time and programming labor which prevents one from reaching arbitrarily high orders.

The program based upon the two-point-renormalization theory is particularly powerful and well suited for our purposes because it becomes technically feasible to incorporate the complexities necessary for treatment of the two tricritical Ising models, whereas other methods of obtaining the series would prove impractical. The two models require (i) the presence of both a finite external field and (ii) the modifications needed to include the directional anisotropy of the exchange of the meta model or the next-nearest-neighbor bonds of the nnn model. These latter complications mainly affect the geometrical details of how the lattice is set up at the beginning of the program. One need only feed in values for the respective exchange constants as input parameters and the iteration proceeds as for the simpler nn isotropic model since the same basic equations apply. Naturally, the computation time increases, as the program must separately keep track of graphs formed of in-plane and out-of-plane bonds in the meta case, and in the nnn model cope with all the extra graphs made possible by second-neighbor bonds.

The essential modifications necessary to go from zero field to finite field are the inclusion of more elementary diagrams and the redefinition of the "bare semi-invariants."[41] In the zero-field case, one has for the Ising model a number of simplifying rules concerning which diagrams make a nonzero contribution to $C_2(\vec{r})$. If the two points between which the correlation function is being evaluated are called the "external" vertices, and the other vertices of the graph are called "internal," then in zero field there is required to be an even number of lines impinging upon an internal vertex and an odd number at the external vertices (where in effect an extra "ghost" line is present). These rules stem from the fact that $\mathrm{Tr} s_i$ vanishes, but may also be understood in terms of the semi-invariants which arise in a linked-cluster expansion. Each vertex in a graph has associated with it a particular semi-invariant corresponding to the number of lines coming into that vertex. Of course, in a vertex-renormalized theory, renormalized semi-invariants are used, as these include contributions from all diagrams which can be constructed from the original skeleton by hanging on "loose ends." All single-particle properties *such as interaction with an external magnetic field* are incorporated in the bare semi-invariants defined as the start of the iteration. The bare semi-invariant of order n, $M_n^{(0)}(h) \equiv M_n^0(\beta\mu H)$, is defined by

$$M_n^{(0)}(h) \equiv \frac{d^n \ln Z_0(h)}{dh^n}, \tag{3.1}$$

where Z_0 is the noninteracting partition function,

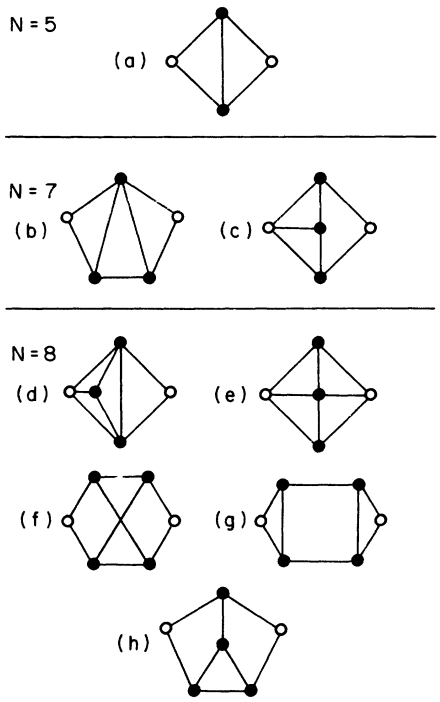

FIG. 3. Eight elementary diagrams needed in finite-field expansion of the two-spin correlation function to eighth order in inverse temperature. The diagrams are grouped by the number of lines N they contain. External vertices are shown as open circles, internal vertices as solid circles. Not counted as separate diagrams are those differing only by an interchange of the external vertices.

$$Z_0 \equiv \mathrm{Tr} e^{\beta\mu H s_i} = \mathrm{Tr} e^{h s_i} = 2\cosh h\,. \tag{3.2}$$

Thus $M_1^{(0)} = \tanh h$, $M_2^{(0)} = 1 - \tanh^2 h$, etc. From (3.1) and (3.2) it is obvious that for $H = 0$ all semi-invariants for odd i vanish, which accounts for the special zero-field rules. In finite field, however, these semi-invariants are nonzero and one must consider all graphs without respect to even-oddness properties.

There are a total of eight elementary diagrams with the number of lines less than or equal to eight, and these are shown in Fig. 3 below. In finite field a diagram first makes a nonzero contribution at the order in inverse temperature equal to the number of lines in the diagram, provided it can be embedded on the lattice. Thus, in general, there are already eight elementary diagrams which must be included in a finite-field calculation to eighth order. By contrast, in zero field to the same order, because of the even-odd rules, only diagram (a) of Fig. 3 need be considered! Indeed, even for a tenth-order calculation in zero field, the only contributing elementary diagrams are the first five, Fig. 3(a)–3(e), plus another one with nine lines [formed from Fig. 3(d) by the addition of a line connecting the external vertex with two impinging lines to the internal vertex with three impinging lines].

The external field is carried along in the semi-invariants as a polynomial in the variable $\tanh(h) = \tanh\beta\mu H$. The resulting expansions for each correlation function $C_2(\vec{r})$ in the high-temperature variable β have, as the coefficient of the β^n term, a polynomial of degree $(n+1)$ in the variable $\tanh^2(h)$. This is an extremely advantageous feature for our various Ising-model series, since it means that once the general field polynomials in $\tanh^2(h)$ are known, we can evaluate the dependence of the external field *exactly* by fixing h and summing the polynomial at each order in β.

In this work we have concentrated not upon the correlation functions themselves[44] but upon the thermodynamic quantities derived from them, reduced susceptibility $\bar{\chi}$ and reduced *staggered* susceptibility $\bar{\chi}_{\mathrm{st}}$. From the fluctuation-susceptibility theorem, we obtain

$$\bar{\chi} = \frac{k_B T \chi}{N\mu^2} = \sum_{\vec{r}} C_2(\vec{r}) \tag{3.3}$$

and

$$\bar{\chi}_{\mathrm{st}} = \frac{k_B T \chi_{\mathrm{st}}}{N\mu^2} = \sum_{\vec{r}} \eta_{\vec{r}}\, C_2(\vec{r})\,. \tag{3.4}$$

For the meta model, the index $\eta_{\vec{r}}$ is $+1$ for sites on even-numbered planes and -1 for odd-numbered planes, since here the two sublattices are the two interpenetrating sets of alternating planes of spins. For the nnn model, $\eta_{\vec{r}}$ is $+1$ if the sum of the Cartesian coordinates $x+y+z$ of point $\vec{r} = (x, y, z)$ is even and -1 if it is odd. To determine the general-field coefficients for $\bar{\chi}$ and $\bar{\chi}_{\mathrm{st}}$, one needs series for a minimum of ten different values of h, so that a 10×10 system of simultaneous linear equations may be solved. Some care is required in the choice of the different h's to optimize the conditions for the solution. The coefficients a_n and b_n for the meta model with $J_{xy} = 1$, $J_z = -1$ are presented in Table I, below, where a_n and b_n are the coefficients through order $n = 8$ in the susceptibility and staggered susceptibility series, respectively,[45]

$$\bar{\chi} = \sum_{n=0}^{\infty} a_n [\tanh(\beta J_{xy})]^n\,, \tag{3.5}$$

$$\bar{\chi}_{\mathrm{st}} = \sum_{n=0}^{\infty} b_n [\tanh(\beta J_{xy})]^n\,. \tag{3.6}$$

The computer time involved to generate series directly from the main program for the many different values of h needed to study the phase boundary would become prohibitive, but the general field expressions allow further series to be obtained with relatively little cost.

There are many possible sources of error in the programming, and checks on the computer code

were essential. As emphasized earlier, we needed a "package" capable of calculating series with both finite field and appropriate lattice modifications present *simultaneously*.

To ensure that the finite field was programmed correctly, we first considered series in a field for nearest-neighbor isotropic lattices. Our results for these cases were matched against results obtained from the data of Gaunt and Baker[19] who give "double" series expansions for h as a function of M and β. We reverted these polynomials to yield M as a double series in H and β, from which the series for susceptibility $\chi = (\partial M/\partial H)$ were derived and compared with those from our program.

A much weaker check was to set $h = 0$ and regain the zero-field series, well known[46] for the various nn isotropic lattices. Further, for an infinite external field $h = \infty$, all correlation functions (and hence $\bar{\chi}$ and $\bar{\chi}_{st}$) vanished to all orders, as expected.

The numerous checks on the modifications for lattice anisotropy and next nearest neighbors are totally independent of those for the finite-field implementation. Rather strong tests on the lattice-programming aspects were provided by having the program reproduce known series in various limits. For example, when $J_2/J_1 \to \infty$ on an fcc lattice, the lattice reduces to bcc, and one obtains the appropriate bcc series.

The strongest test on the correctness of the whole package for either the meta or nnn model is performed by summing the general-field coefficients for any order in β in both the $\bar{\chi}$ and $\bar{\chi}_{st}$ series. These coefficients were obtained from correlation-function data from runs for at least ten different values of h with the required lattice anisotropy or nnn bonds already built into the program. The sum should be zero, since $\tanh^2(h) = 1$ when $h = \infty$, for which both χ and χ_{st} vanish to all orders. The numbers in Table I indeed satisfy this check and so do the nnn model series reported in Paper II.

IV. RESULTS FOR CRITICAL LINE AND CONFIRMATION OF SMOOTHNESS POSTULATE

As discussed in Sec. II, the strongly divergent quantity along the second-order line of an antiferromagnet is the staggered susceptibility χ_{st}, analogous to the strongly divergent direct susceptibility at the Curie point of a ferromagnet. The smoothness postulate or universality hypothesis predicts that as long as the transition remains second order, we will expect

$$\bar{\chi}_{st} \sim [T - T_c(H)]^{-5/4}. \tag{4.1}$$

Using the general-field expansions for $\bar{\chi}_{st}$ determined by the methods described in Sec. III, we have mapped out the critical line in the H-T plane and examined the universality prediction. Our

TABLE I. Coefficients a_n and b_n through order $n = 8$ in the meta-model series for the susceptibility and staggered susceptibility, Eqs. (3.5) and (3.6), respectively. Here the expansion variable X denotes $\tanh^2 h \equiv \tanh^2(\mu H/k_B T)$. A single asterisk denotes an uncertainty in the last digit; two asterisks denote an uncertainty in the last two digits.

$a_0 = 1 - X$	$b_0 = 1 - X$
$a_1 = 2 - 8X + 6X^2$	$b_1 = 6 - 16X + 10X^2$
$a_2 = -2 + 2X + 10X^2 - 10X^3$	$b_2 = 30 - 134X + 186X^2 - 82X^3$
$a_3 = -14 + 200X - 566X^2 + 576X^3 - 196X^4$	$b_3 = 150 - 880X + 1894X^2 - 1760X^3 + 596X^4$
$a_4 = -42 + 1026X - 5144X^2 + 10\,040X^3 - 8526X^4 + 2646X^5$	$b_4 = 726 - 5150X + 14\,600X^2 - 20\,536X^3 + 14\,258X^4 - 3898X^5$
$a_5 = -46 + 1960X - 16814X^2 + 56\,256X^3 - 88\,048X^4 + 65\,040X^5 - 18\,348X^6$	$b_5 = 3510 - 28\,848X + 99\,166X^2 - 182\,208X^3 + 188\,208X^4 - 103\,296X^5 + 23\,468X^6$
$a_6 = -90 - 1014X + 10434X^2 - 594X^3 - 105\,900X^4 + 237\,436X^5 - 200\,228X^6 + 59\,956X^7$	$b_6 = 16\,710 - 157\,342X + 635\,378X^2 - 1\,426\,906X^3 + 1\,924\,948X^4 - 1\,559\,284X^5 + 701\,564X^6 - 135\,068X^7$
$a_7 = 2 - 19\,304X + 320\,862X^2 - 1\,757\,952X^3 + 4\,597\,716X^4 - 6\,479\,120X^5 + 5\,015\,212X^6 - 1\,984\,256X^7 + 306\,840X^8$	$b_7 = 79\,494 - 843\,728X + 3\,932\,594X^2 - 10\,493\,024X^3 + 17\,509\,596X^4 - 18\,699\,904X^5 + 12\,478\,036X^6 - 4\,755\,072X^7 + 792\,008X^8$
$a_8 = -1402 - 28\,478X + 1\,155\,680X^2 - 10\,011\,488X^3 + 40\,107\,912X^4 - 88\,872\,520X^5 + 115\,745\,632{*}X^6 - 88\,314\,336{**}X^7 + 36\,561\,936{**}X^8 - 6\,342\,936{**}X^9$	$b_8 = 375\,174 - 4\,445\,438X + 23\,579\,488X^2 - 73\,392\,864X^3 + 147\,460\,232X^4 - 197\,953\,224X^5 + 177\,251\,104{*}X^6 - 101\,949\,760{**}X^7 + 34\,145\,680{**}X^8 - 5\,070\,392{**}X^9$

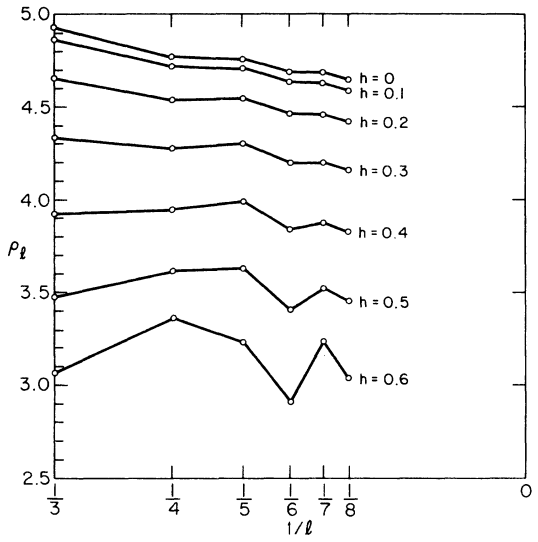

FIG. 4. Ratio plots ρ_l vs $1/l$ for staggered susceptibility series at various values of $h \equiv \mu H/kT$ [cf. Eqs. (4.3) and (4.4)]. Note the presence of oscillations in the ratios.

analysis of the series employs the usual ratio and Padé-approximant (PA) methods.[47] Although series convergence worsened for higher values of field, we believe our results provide good evidence for universality for a wide range of the external field.

To emphasize the dependence of the coefficients of a given series upon the particular $h \equiv \mu H/k_B T$ path it is computed along, we write

$$\bar{\chi}_{st}(h) = \sum_{l=0}^{\infty} b_l(h)\beta^l . \tag{4.2}$$

These paths are "rays" through the origin in the H-T plane and have the property that they must intersect the critical line lying in this plane somewhere along their length, at least when the transition is second order.[48] Our series will continue to exhibit singularities below the TCP where the transition becomes first order, but they cannot be used to locate the first-order line. Indeed, our initial estimate of the location of the TCP relies upon the unphysical hooking upward or downward of the calculated phase boundary observed beyond a certain value of h.

The ratio and PA analysis will be discussed in turn.

A. Ratio Method

In the ratio method, we form the ratios of successive series coefficients of Eq. (4.2),

$$\rho_l(h) \equiv b_l(h)/b_{l-1}(h) , \tag{4.3}$$

and plot these vs $1/l$ for various values of h. If the series is dominated by a singularity of the form $\bar{\chi}_{st}(h) \sim [T - T_c(h)]^{-\gamma_{st}}$, we expect[47] the ratios to settle down to the form

$$\rho_l(h) = k_B T_c(h)[1 + (\gamma_{st} - 1)/l] , \tag{4.4}$$

where universality predicts that γ_{st} is independent of h.

It is seen that the ratios of Fig. 4 have oscillations characteristic of loose-packed lattices (sc with nn bonds only). Such oscillations generally arise from the presence of one or more interfering singularities in the complex temperature plane,[49] and in this model, in particular, they are due to a pole on the negative real axis. This may be understood in zero field as due to the weak singularity in the staggered susceptibility for the ferromagnet obtained by changing the sign of J_z, just as the susceptibility for a two-sublattice ferromagnet shows a weak antiferromagnetic singularity.[50] The negative pole should occur at precisely $-T_N$, since flipping all spins on one sublattice and changing the sign of J_z simultaneously leaves the Hamiltonian invariant. While this symmetry no longer holds in finite field, the log Padé tables, from which the distribution of poles may be gauged, indicate that the negative real pole persists at small fields and then gradually gets smeared out as complex poles begin to enter at higher fields.

To improve the convergence of the $\bar{\chi}_{st}$ series and diminish the effects of the interfering singularities, we carried out a bilinear transformation[49,51] on the original high-temperature variable β to give a new expansion variable β^*,

$$\beta^* \equiv \beta/(1 + c\beta) . \tag{4.5}$$

Note that $c = 0$ corresponds to a series with the original coefficients. The ratio plots for the transformed series with the choice $c = 1$ for the same set of h values as in Fig. 4 are shown in Fig. 5. The ratios now lie on much straighter lines, and afford estimates for the critical temperature from the intercept at $1/l = 0$ and the exponent γ_{st} from the slope. Successive estimates for the critical temperature, here a function of both path h and transformation parameter c, are given by

$$k_B T_c^{(l)}(h, c) = l\rho_l(h, c) - (l-1)\rho_{l-1}(h, c) , \tag{4.6}$$

where the transformed critical temperature is trivially related to the true critical temperature through Eq. (4.5) by $k_B T_c(h, c) = k_B T_c(h, 0) + c$. A sequence of estimates for the exponent may be formed,

$$\gamma_{st}^{(l)}(h, c) = 1 - l\left(1 - \frac{\rho_l(h, c)}{k_B T_c^{(l)}(h, c)}\right) . \tag{4.7}$$

In principle, γ_{st} will be asymptotically ($l \to \infty$) unaffected by the bilinear transformation, but in practice, with a finite number of terms, the values of γ_{st} vary slightly with c. Of course, once one has a "best" estimate for T_c, this may be used in

TABLE II. Estimates of exponents γ_{st} and critical temperatures T_c for various values of $h \equiv \mu H/k_B T$ and for various values of bilinear transformation parameter c. Here γ_{st}^R and $k_B T_c^R$ are determined from the slope and intercept of the line joining the final two points on the ratio plot, ρ_7 and ρ_8 [cf. Eqs. (4.6) and (4.7)]. Note $c=0$ corresponds to the untransformed original series, whose irregularity did not permit reliable estimates using ratio plots. The entry $k_B T_c^P$ is the singularity estimated from Padé approximants to the series $[\bar{\chi}_{st}(h,c)]^{4/5}$. The two entries represented by three dots denote insufficient convergence to allow an estimate from the Padé table.

	$c=0$	$c=1.0$			$c=1.5$			$c=2.0$		
h	$k_B T_c^P$	γ_{st}^R	$k_B T_c^R$	$k_B T_c^P$	γ_{st}^R	$k_B T_c^R$	$k_B T_c^P$	γ_{st}^R	$k_B T_c^R$	$k_B T_c^P$
0	4.51	1.25	4.51	4.51	1.23	4.52	4.51	1.22	4.52	4.51
0.1	4.45	1.26	4.45	4.46	1.24	4.46	4.46	1.22	4.47	4.46
0.2	4.29	1.28	4.27	4.29	1.25	4.28	4.30	1.23	4.30	4.29
0.3	4.04	1.30	4.00	4.04	1.27	4.02	4.04	1.24	4.04	4.04
0.4	3.73	1.29	3.69	3.73	1.28	3.70	3.73	1.24	3.72	3.72
0.5	3.37	1.22	3.37	3.38	1.25	3.34	3.37	1.23	3.36	3.37
0.6	...	1.05	3.07	3.01	1.21	2.99	3.01	1.25	2.97	3.01
0.7	...	0.86	2.80	2.67	1.26	2.60	2.67	1.46	2.49	2.67

Eq. (4.7) to produce a new sequence of estimates for γ_{st}.

Table II lists estimates for the critical temperature and exponent determined by Eqs. (4.6) and (4.7), respectively, for eight field values and three different values of transformation parameter c. They are the final estimates $kT_c^{(8)}$ and $\gamma_{st}^{(8)}$ obtained from the line joining the last two points on the ratio plot, ρ_7 and ρ_8. Also shown are estimates $k_B T_c^P$ from Padé approximants, to be discussed below. Using $kT_c^{(8)}$ as the best estimate for the critical temperature, one may recalculate the sequence $\gamma_{st}^{(l)}$ by passing lines through the points ρ_l and $k_B T_c^{(8)}$. The set $\gamma_{st}^{(l,8)}$ obtained in this manner from the transformed series with $c=1.5$ and various field values are shown in the $1/l$ plots of Fig. 6. Note $\gamma_{st}^{(8,8)}$ is not shown since it is identical to $\gamma_{st}^{(7,8)}$.

B. Padé Approximants

When both the exponent and critical temperature of a series are unknown, the method of log Padés may be applied. This refers to the operation of forming the PA to the logarithmic derivative of a series expansion of some function $f(\beta)$ expected to vary like $f(\beta) \sim (\beta_c - \beta)^{-\lambda}$. Then,

$$g(\beta) \equiv \frac{d}{d\beta} \ln f(\beta) \sim \frac{\lambda}{\beta_c - \beta} \tag{4.8}$$

and the PA's to the new series for $g(\beta)$ might be expected to represent this function well and show poles at $\beta = \beta_c$ with a residue of $-\lambda$. An interfering singularity such as β_c' of strength λ' should also be represented, provided it entered f as a multiplicative factor in the form $(\beta_c - \beta)^{-\lambda}(\beta_c' - \beta)^{-\lambda'}$.

We applied this method to the $\bar{\chi}_{st}$ series along numerous field paths, and a sample of the results

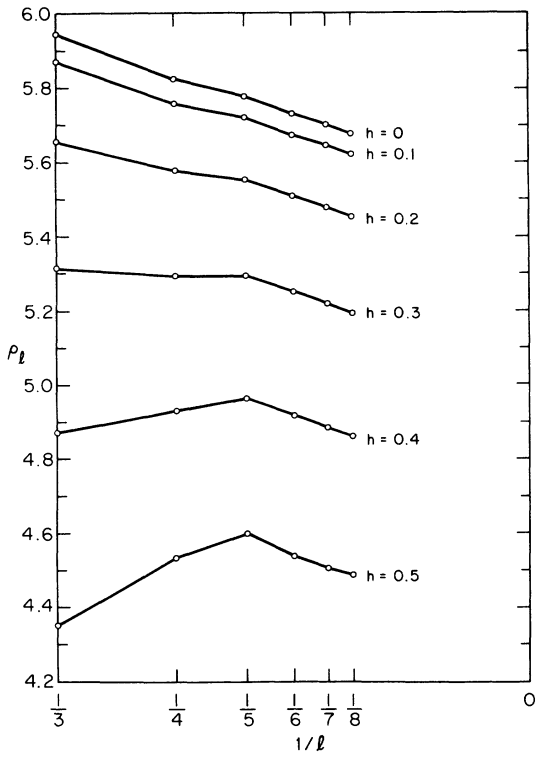

FIG. 5. Ratio plots for $\bar{\chi}_{st}$ series at various field values after transformations of the high-temperature expansion variable from $\beta \equiv 1/k_B T$ to $\beta^* \equiv \beta/(1+\beta)$ [cf. Eq. (4.5)]. The oscillations of Fig. 4 have been "ironed out," allowing estimates of the critical temperature $k_B T_c(h)$ from the respective intercepts and the exponent γ_{st} from the slopes.

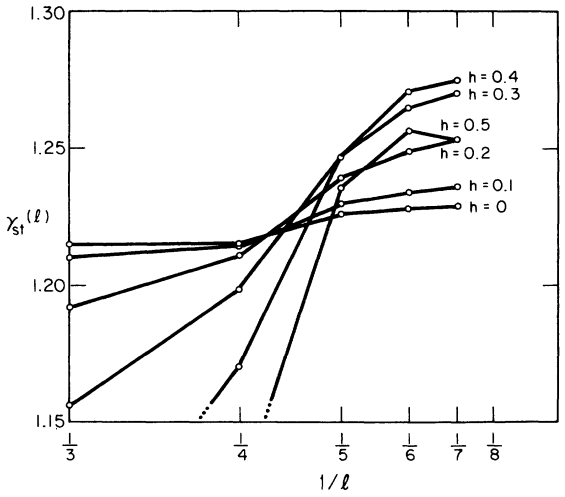

FIG. 6. Ratio-method sequence of estimates $\gamma_{st}^{(l)}$ vs $1/l$ for various field values [cf. Eq. (4.7)]. Here $k_B T_c^{(8)}(h)$ has been taken as the best estimate of the critical temperature, and a value for the bilinear transformation parameter of $c=1.5$ has been used [see discussion in text and Eq. (4.5)].

is presented in Table III. In each Padé table the entries for the physical pole $k_B T_c$, and the corresponding residue, are given. It is clear that, except perhaps for the $h=0$ case, the tables do not have sufficient convergence to produce conclusive results regarding $k_B T_c(h)$ or γ_{st}, with convergence worsening for higher fields. Considerably longer series are probably required to make the log-Padé method profitable here.

PA's were employed with considerably more success in locating the critical temperature as a function of field when the exponent γ_{st} was fed into the series as a known quantity. Here a given

TABLE III. Log Padé tables for $\bar{\chi}_{st}$ series along various h paths. In parentheses below each pole is the corresponding residue. The notation ··· denotes the fact that no physical pole appeared in that entry of the table.

D \ N	1	2	3	4	5
			(a) $h=0$		
2	4.51	4.53	4.51	4.50	4.51
	(1.25)	(1.24)	(1.25)	(1.27)	(1.26)
3	4.52	4.52	4.56	4.50	
	(1.24)	(1.24)	(1.24)	(1.26)	
4	4.51	4.55	4.51		
	(1.25)	(1.23)	(1.25)		
5	4.50	4.50			
	(1.27)	(1.26)			
6	4.51				
	(1.26)				
			(b) $h=0.2$		
2	4.38	4.42	4.34	4.24	4.25
	(1.16)	(1.13)	(1.21)	(1.36)	(1.34)
3	4.41	4.39	···	4.25	
	(1.13)	(1.15)		(1.34)	
4	4.35	···	4.30		
	(1.20)		(1.24)		
5	4.22	4.24			
	(1.40)	(1.37)			
6	4.24				
	(1.37)				
			(c) $h=0.4$		
2	4.11	4.10	3.90	3.61	3.70
	(0.86)	(0.87)	(1.06)	(1.53)	(1.31)
3	4.10	4.11	···	3.67	
	(0.87)	(0.86)		(1.39)	
4	4.09	4.30	3.77		
	(0.87)	(0.81)	(1.17)		
5	···	3.48			
		(2.26)			
6	3.59				
	(1.62)				

TABLE IV. Singularities given by Padé-approximant tables to $(\bar{\chi}_{st})^{4/5}$ for various h paths. Thus the numbers shown should be approximating the critical temperature $T_c(h)$.

D \ N	1	2	3	4	5	6
			(a) $h=0$			
2	4.52	4.51	4.51	4.51	4.51	4.51
3	4.51	4.51	4.51	4.51	4.51	
4	4.51	4.51	4.51	4.51		
5	4.51	4.52	4.51			
6	4.51	4.51				
7	4.51					
			(b) $h=0.2$			
2	4.23	4.28	4.30	4.31	4.30	4.29
3	4.28	4.69	4.31	4.31	4.28	
4	4.30	4.31	4.30	4.29		
5	4.31	4.30	4.29			
6	4.30	4.28				
7	4.29					
			(c) $h=0.4$			
2	3.43	3.76	3.63	3.78	3.72	3.72
3	3.69	3.89	3.79	3.76	3.72	
4	3.69	3.75	3.72	3.73		
5	3.74	3.73	3.73			
6	3.73	3.73				
7	3.73					

$\bar{\chi}_{st}(h)$ series is raised to the $\frac{4}{5}$ power and a Padé analysis done on the resulting series. Universality predicts $\bar{\chi}_{st} \sim A(T_c)[T - T_c(H)]^{-5/4}$, where the amplitude is now explicitly displayed; if this holds, the new series $\bar{\chi}_{st}^{4/5}$ should have a simple pole at $T_c(H)$, visible in the denominators of the PA's. These are now PA's whose degree $N+D \leq 8$, the full order of the original series, and whose residues at the poles are the amplitude $[A(T_c)]^{4/5}$. The log-Padé tables are of one degree less ($N+D \leq 7$) because of the differentiation with respect to the expansion variable. We defer a discussion of the behavior of the amplitude $A(T_c)$ along the phase boundary to Paper II, where a tricritical-point scaling hypothesis is used to make theoretical predictions for the variation of the amplitude.

This procedure was carried out both on the series in their original expansion variable, and on the transformed series. Table IV shows a few of the $c=0$ Padé tables, and estimates of critical temperatures from the $c=0$ PA's and estimates from the PA's for the $c=1.0$, 1.5, and 2.0 cases are listed under $k_B T_c^P$ in Table II. We note the excellent consistency among the various Padé estimates for a given path h. Further, there is very good agreement between the Padé estimates for T_c and those from the ratio method; for values of h up to 0.5, there is never more than a 1% discrepancy. Comparison of $k_B T_c^R(h)$ and $k_B T_c^P(h)$ for h up

to 0.4 reveals the general pattern that when $T_c^R < T_c^P$, then $\gamma_{st}^R > \frac{5}{4}$, and when $T_c^R > T_c^P$, $\gamma_{st}^R < \frac{5}{4}$.

The $T=0$ critical field $\mu H_c(0)$ may be easily calculated exactly for this model by equating the energies of a lattice of perfectly ordered planes with spins opposite on adjacent planes in an external field H_c (cf. Fig. 2) to the energy of a lattice with all spins pointing up under the influence of H_c. This gives

$$\mu H_c(0) = q_z |J_z|, \tag{4.9}$$

where q_z is the coordination number in the z direction. For the parameters we have chosen, $\mu H_c(0) = 2 \times 1 = 2$.

Several factors lead us to conclude that Table II provides strong evidence for the universality prediction of $\gamma_{st} = \frac{5}{4}$ for a wide range of field values. The values for γ_{st}^R predicted by ratio methods from the various transformed series are closely scattered on either side of $\frac{5}{4}$ for values of h up to $h \cong 0.5$. This h corresponds to a critical field of $\mu H_c \cong 0.5(3.4) = 1.7$, a substantial fraction of the maximum $T=0$ critical field of 2. Further, there is quite good agreement between the ratio and Padé predictions for T_c. The T_c^P are singularities whose location is predicted upon the assumption of a $\frac{5}{4}$ power-law divergence. If in fact the $\bar{\chi}_{st}(h)$ series did not diverge with this power, neither such agreement with the T_c^R, nor even a well-convergent PA, would be expected. The PA's on the transformed series continued to converge to singularities for the higher-field values for which the ratios were less consistent, and, as can be seen from Table II, the agreement among the T_c^P for the three values of c remains excellent.

The scatter of the γ_{st}^R about 1.25 and the small discrepancies between T_c^R and T_c^P are due, we believe, to insufficient convergence of the series. The trend in the ratio-plot results remarked upon earlier is consistent with what might be expected from the ratio plot for a series which has not, in some sense, fully converged. That is, low estimates of T_c are associated with high estimates for γ_{st}, while high estimates of T_c go with low estimates for γ_{st}. Obviously, information from a finite number of terms is limited, and longer series are always useful.

We used the points (T_c, H_c) obtained from the PA's to the $\bar{\chi}_{st}(h; c=1)$ series to obtain the phase boundary shown in Fig. 7. The value of h was stepped by 0.02 for each successive point, but lack of space forbids a complete tabulation of the calculated critical temperatures and fields. The Padés along steeper and steeper h paths continue to show singularities which are obviously unphysical beyond a certain point, for the critical line hooks up and to the right to give critical fields greater than the maximum $T=0$ value of 2, and double-valued critical fields for a given temperature. This behavior is attributed to the fact that the series are here probing the first-order region, and are unable to locate the first-order phase boundary. We specu-

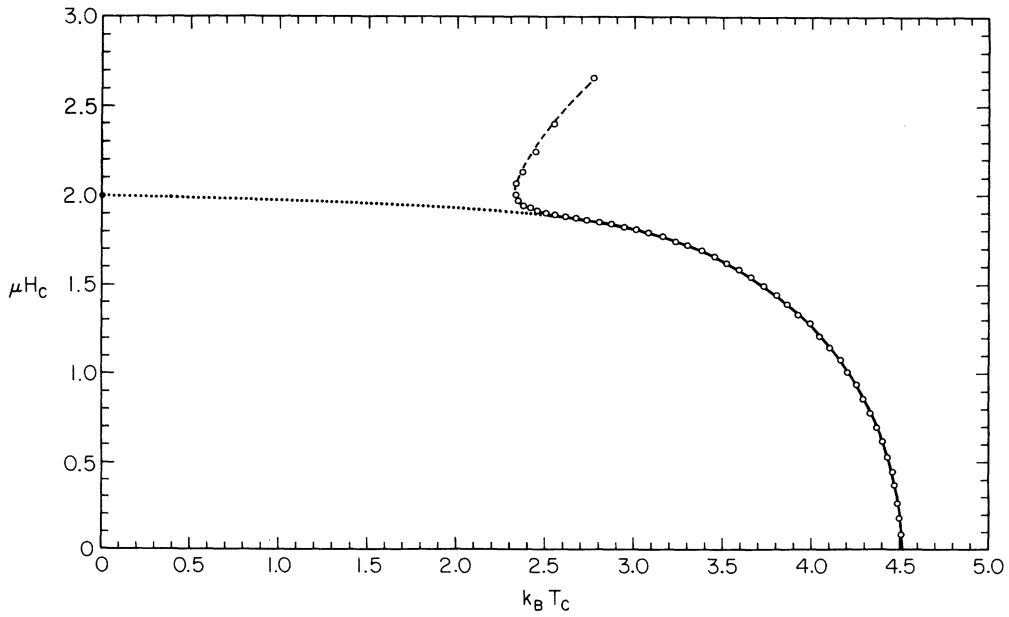

FIG. 7. Phase boundary for meta model of Eq. (2.3) with $J_{xy}=1$, $J_z=-1$. The second-order portion of the phase line is shown solid, the first-order portion is shown dotted, while the spurious hooking near the tricritical point is shown dashed.

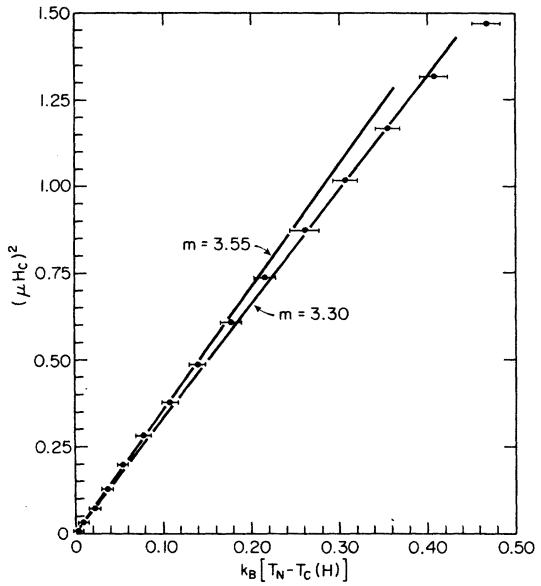

FIG. 8. Plot of square of critical field $(\mu H_c)^2$ vs $k_B[T_c(H) - T_N]$, the deviation of critical temperature from the Néel point. The mean-field theory predicts $(\mu H_c)^2 = 3.55\ k_B[T_c(H) - T_N]$, and a line of slope $m = 3.55$ is seen to provide an excellent fit to the series data for low fields. The error bars for each point give some measure of the uncertainty from the series-extrapolation estimates. Also shown for comparison is a line of slope $m = 3.30$.

late that perhaps the series in this region are responding to singularities of the wings, which may lie very close to the H-T plane.

To locate the TCP approximately, we draw a curve from the $T = 0$ critical-field point to join the calculated phase line smoothly, i.e., we assume the first- and second-order lines are asymptotically parallel to the TCP. The TCP vicinity then falls at $k_B T_c \cong 2.60 (h \cong 0.72)$. In Sec. V, we describe how matching the singularities between the $\bar{\chi}_{st}$ and $\bar{\chi}$ series in this neighborhood locates the TCP with greater precision and furnishes an estimate for the tricritical susceptibility exponent $\bar{\gamma}$.

C. Mean-Field-Theory Predictions

Not surprisingly, mean-field theory overestimates the ordering temperature. The MFT prediction[30] for the Néel temperature is $k_B T_N^{(MF)} = q_{xy} J_{xy} + q_z |J_z|$, where q_{xy} is the coordination number in the xy plane, and q_z is as defined before. Thus $k_B T_N^{(MF)} = 6$ in the present problem, while series give $k_B T_N^{(ser)} \cong 4.51$. Although the absolute temperatures differ, the MF prediction for the *shape* of the phase boundary near T_N is in remarkable agreement with the series-calculation results. According to MF theory, the phase boundary obeys the square-root law

$$\mu H_c = 2 q_z |J_z| \left(\frac{T_N - T_c}{T_N} \right)^{1/2}, \tag{4.10}$$

which yields $(\mu H_c)^2 = 3.55 k_B (T_N - T_c)$ upon substitution of $q_z = 2$, $|J_z| = 1$, and $k_B T_N \cong 4.51$. A plot of our series values for $(\mu H_c)^2$ vs $k_B(T_N - T_c)$ is shown in Fig. 8. A line of slope 3.55 is seen to be well within the approximate errors bars indicated for each point (determined from the degree of convergence of the PA's) for fields up to $\mu H_c \simeq 1$.

V. RESULTS FOR THE TRICRITICAL POINT AND ESTIMATE OF TRICRITICAL SUSCEPTIBILITY EXPONENT

We now consider in greater detail what was identified in the previous section as the tricritical region and turn our attention to the direct susceptibility series. We discussed in Sec. II how the susceptibility $\bar{\chi}$ may be expected to be more strongly divergent at the TCP than along the critical line. It is therefore anticipated that the $\bar{\chi}$ series have the following two properties:

(a) Their Padé tables are reasonably well convergent in the vicinity of the TCP; (b) the singularity they exhibit near the TCP matches the singularity obtained from the $\bar{\chi}_{st}$ series along the same h path.

In our analysis of the $\bar{\chi}_{st}$ series in Sec. IV, we located the critical line and its spurious continuation beyond the TCP. Observation of where the unphysical behavior of the critical line begins, and continuation of the phase boundary to $T = 0$, furnishes an approximate location of the TCP. An independent method for its location is the criterion of matching singularities between the two different series $\bar{\chi}$ and $\bar{\chi}_{st}$. Using this criterion, we confirm with greater precision the TCP locations of Sec. IV and, further, obtain estimates for the tricritical susceptibility exponent $\bar{\gamma}_{meta}$. Adding considerably to our confidence was the independent confirmation of the location of the TCP by Monte Carlo calculations.[29]

The $\bar{\chi}$ series are extremely irregular in the vicinity of $h \simeq 0.72$, identified as the tricritical region in Sec. IV. The coefficients of the series are both positive and negative in no obvious pattern,

TABLE V. Singularities given by PA's to the series $[\bar{\chi}_{st}(h = 0.72)]^{4/5}$. The critical temperature is estimated to be $k_B T_c = 2.60 \pm 0.05$.

D \ N	2	3	4	5	6
2	3.42	2.91	3.12	2.59	2.60
3	2.60	2.15	2.67	2.60	
4	...	2.51	2.62		
5	2.57	2.60			
6	2.62				

TABLE VI. Singularities given by log Padé method to $\bar{\chi}(h=0.72)$ series. Notation as before in Table III.

D \ N	1	2	3	4	5
2	...	...	...	...	...
3	...	2.53 (0.59)	2.35 (0.77)	3.55 (0.10)	
4	...	2.32 (0.83)	2.51 (0.61)		
5	...	3.05 (0.26)			
6	...				

and are not monotonically increasing in absolute value. The actual series for $\bar{\chi}$ along $h=0.72$ is

$$\bar{\chi}(0.72) = 0.619\,423 - 0.175\,583\beta - 0.341\,680\beta^2 + 7.83\,386\beta^3 - 0.658\,673\beta^4 - 25.8028\beta^5 + 138.652\beta^6 + 64.8752\beta^7 - 541.644\beta^8. \quad (5.1)$$

The ratio method is useless on such badly behaved series.

The PA to the $(\bar{\chi}_{st})^{4/5}$ series along $h=0.72$ is shown in Table V. It appears to show a singularity at $k_BT_c \sim 2.60$, with only fair convergence. The log Padé to the $\bar{\chi}$ series along the same path resulted in Table VI, which evidently does not converge well and is fairly inconclusive. However, at least some of the entries ($[D, N]=[3, 2], [4, 3]$) are compatible with the singularity indicated by the $\bar{\chi}_{st}$ series. The residues at these poles are $\simeq 0.6$, and clearly the higher values for the poles in the table are associated with lower residues. Thus, while far from being strong evidence, the log-Padé table provides at least a suggestion of a value for $\bar{\gamma}_{meta} \lesssim 0.6$, perhaps something near 0.5 for a critical temperature $k_BT_c \cong 2.60$. We will see in Paper II that the log-Padé table for the nnn $\bar{\chi}$ series has much better convergence and is able to furnish a more definite estimate for $\bar{\gamma}_{nnn}$.

In the next stage of analysis we raise the $\bar{\chi}(h=0.72)$ series to a variety of powers and do a full *eighth*-order Padé on the resulting series. That is, we calculate the PA to $\bar{\chi}^p$, where p is varied. It was expected that the $\bar{\chi}$ series raised to the inverse of a power close to the correct $\bar{\gamma}_{meta}$ would show a reasonably well-convergent Padé table, with a pole reproducing the pole from the $\bar{\chi}_{st}$ analysis ($k_BT_c \cong 2.60$ for $h=0.72$). Motivated by the log-Padé results, we tried values for p corresponding to values of $\bar{\gamma}_{meta}$ near 0.5, i.e., $p \cong (0.5)^{-1} = 2$.

We show in parts (a)–(c) of Table VII, the PA's to the series $\bar{\chi}(0.72)$ raised to powers p equal to the inverse of 0.4, 0.5, and 0.6, respectively. For $p=2.5$, the singularity appears at $k_BT_c \cong 2.67$, for $p=2$, at $k_BT_c \cong 2.58$, and for $p=\frac{5}{3}$, at $k_BT_c \cong 2.52$. The critical temperature from the $\bar{\chi}^2$ series is seen to be the closest to the value predicted from the $\bar{\chi}_{st}$ PA of Table V. The two singularities from Tables VII (b) and Table V lie within 1% of each other, and well within the admittedly somewhat subjective error bars assigned to each on the basis of the extent of Padé convergence. Moreover, if the three tables (a)–(c) are compared with respect to convergence, the convergence of the $\bar{\chi}^2$ case is seen to be rather good, being slightly better than the convergence of the $\bar{\chi}^{5/3}$ Padé and much better than for the $\bar{\chi}^{5/2}$ Padé.

The $\bar{\chi}$ series along other paths in the neighborhood of $h=0.72$ were subjected to similar raising to various powers. The $\bar{\chi}^{5/2}$ series always showed slightly greater critical temperatures than the $\bar{\chi}_{st}$ series, the $\bar{\chi}^{5/3}$ series showed definitely lower critical temperatures, while the $\bar{\chi}^2$ series showed best consistency with the $\bar{\chi}_{st}$ results, particularly in the $h=0.70-0.74$ region. Further away from the $h=0.72$ path, the mutual consistency of the two roots from the $\bar{\chi}^2(h)$ and $\bar{\chi}_{st}(h)$ PA's worsened, as did the convergence of the $\bar{\chi}^2(h)$ PA itself. Powers different from two produced nonconvergent PA's and/or singularities even further removed from the corresponding $\bar{\chi}_{st}$ singularity.

For the purposes of illustration, we give in Tables VIII and IX the same data as were presented in

TABLE VII. Singularities given by Padé approximants to $[\bar{\chi}(h=0.72)]^p$, with (a) $p=\frac{5}{2}$, (b) $p=2$, and (c) $p=\frac{5}{3}$. Convergence and consistency with the $\bar{\chi}_{st}(0.72)$ results are best for the $\bar{\chi}^2$ Padé, part (b), from which the critical temperature is estimated to be $k_BT_c = 2.58 \pm 0.01$.

D \ N	2	3	4	5	6
		(a) $p=\frac{5}{2}$			
2	...	...	...	...	...
3	2.84	2.66	2.70	3.06	
4	...	2.69	2.66		
5	2.76	3.03			
6	2.87				
		(b) $p=2$			
2	...	...	...	...	...
3	2.59	2.58	2.59	2.96	
4	2.58	2.58	2.58		
5	2.59	2.58			
6	...				
		(c) $p=\frac{5}{3}$			
2	...	...	...	...	...
3	2.39	2.52	2.50	2.89	
4	2.48	2.51	2.52		
5	2.50	2.48			
6	2.40				

TABLE VIII. Singularities given by PA's to $[\bar{\chi}(h=0.68)]^p$ with same powers p in parts (a), (b), and (c) as in Table VII.

D \ N	2	3	4	5	6
		(a) $p=\frac{5}{2}$			
2	...	...	...	...	...
3	3.03	2.79	2.80	3.11	
4	...	2.80	2.79		
5	2.92	2.97			
6	2.97				
		(b) $p=2$			
2	...	...	...	...	...
3	2.77	2.68	2.69	3.00	
4	2.63	2.69	2.68		
5	2.70	2.62			
6	2.93				
		(c) $p=\frac{5}{3}$			
2	...	...	...	...	...
3	2.56	2.61	2.61	2.94	
4	2.60	2.61	2.61		
5	2.60	2.60			
6	2.45				

Table VII but along the paths $h=0.68$ and $h=0.76$, respectively. The critical temperatures from the $\bar{\chi}_{st}$ analysis are $k_B T_c(0.68) \cong 2.73$ and $k_B T_c(0.76) \cong 2.50$. Table VIII indicates that again the $\bar{\chi}^2$ series gives a singularity closest to that from $\bar{\chi}_{st}$, although now the $\bar{\chi}^{5/3}$ PA is better convergent. In Table IX, the $\bar{\chi}^2$ series is both the best convergent and gives the closest singularity to that from $\bar{\chi}_{st}$ series.

Assessing, then, the over-all evidence, we corroborate our original estimate of the tricritical region, and put the tricritical path at $h_t \simeq 0.72 \pm 0.02$. This corresponds to a tricritical temperature of $k_B T_t \simeq 2.60$, with error bars of $\lesssim 2\%$, or $T_t/T_N = 0.58 \pm 0.01$. Moreover, we may now estimate the tricritical susceptibility exponent for this model to be $\bar{\gamma}_{meta} \simeq 2^{-1} = \frac{1}{2}$, or

$$\bar{\chi}_{meta} \sim (T - T_t)^{-1/2}, \tag{5.2}$$

with error bars for $\bar{\gamma}_{meta}$ of about 10%, or 0.05. Again, we emphasize that these error bars are to be regarded as somewhat subjective.

The very recent Monte Carlo studies[29] on the same model with precisely the same parameters yield $T_t/T_N = 0.58 \pm 0.01$, and $\bar{\gamma}_{meta} = 0.55 \pm 0.15$, in excellent agreement with our series results. The Monte Carlo calculation was done both along an $H/T = \text{const}$ path, identical to the kind of path we used, and along a constant magnetization path with $M = M_t$, the tricritical magnetization. The latter path should *not* generally be expected to yield the same exponent as an $H/T = \text{const}$ or an $H = \text{const}$ path, since a constant magnetization path is expected to come in asymptotically parallel to the phase boundary and not at a finite angle.[52] However, for technical reasons, such as the $M = M_t$ data perhaps lying outside the "crossover" region, both Monte Carlo paths appear to produce the same exponent.

Comparison with Mean-Field Theory

The MFT prediction for the ratio T_t/T_N for the parameters in this model is

$$\left(\frac{T_t}{T_N}\right)^{MF} = 1 - \frac{q_s |J_s|}{3 q_{xy} J_{xy}} = \frac{5}{6}. \tag{5.3}$$

It is characteristic of MFT to overestimate the ordering present in a system by making every spin interact equally with every other spin through the same effective field. However, in a model with both ferromagnetic- and antiferromagnetic-ordering tendencies, it is difficult to argue in advance how MFT will treat the ratio T_t/T_N. This ratio in some sense measures the relative strength of the ferromagnetic versus antiferromagnetic tendencies in the system. Evidently, in this case MFT amplifies the ferromagnetic order at the expense of the antiferromagnetic order, since we find $(T_t/T_N)^{MF} \gg (T_t/T_N)^{ser}$.

According to MFT, the susceptibility χ is finite at T_t as the TCP is approached from above, i.e., from the high-temperature paramagnetic phase. This prediction, of course, is in direct contrast to Eq. (5.2), and also contradicts what appears to be a divergent χ in experiments on real metamag-

TABLE IX. Singularities given by PA's to $[\bar{\chi}(h=0.76)]^p$, with some powers p in parts (a), (b), and (c) as in Table VII.

D \ N	2	3	4	5	6
		(a) $p=\frac{5}{2}$			
2	...	...	...	...	...
3	2.62	2.52	2.60	3.03	
4	2.47	2.56	2.50		
5	2.60	2.33			
6	2.75				
		(b) $p=2$			
2	...	...	...	...	...
3	2.38	2.47	2.47	2.93	
4	2.45	2.47	2.47		
5	2.47	2.45			
6	...				
		(c) $p=\frac{5}{3}$			
2	...	...	...	...	...
3	2.19	2.43	2.38	2.87	
4	2.34	2.39	2.43		
5	2.37	2.33			
6	2.21				

nets near their TCP's.[4] What happens as T_t is approached from below? Here MFT does in fact predict a divergent χ, but only at the TCP. Along the rest of the second-order phase boundary up to T_N, MFT yields a finite χ as the critical temperature is approached from either above or below.

Tricritical scaling will be discussed for both the meta and the nnn model in Paper II.

ACKNOWLEDGMENTS

The authors are indebted to Professor R. B. Griffiths, Professor M. Wortis, and Professor T. S. Chang for invaluable correspondence and conversations concerning various aspects of this work. Special thanks must go to Professor D. P. Landau, who very kindly and promptly agreed to run his Monte Carlo programs on the meta model. As the authors have emphasized, the agreement between the results obtained by two independent methods of analysis added considerably to their confidence. They are also very grateful for numerous discussions with R. Ditzian, A. Hankey, D. Karo, R. Krasnow, D. Lambeth, M. H. Lee, L. Liu, and G. Paul.

---

*Work forms portion of a Ph.D. thesis to be submitted to the Physics Department of MIT by F. H. Work supported by National Science Foundation, Office of Naval Research, and Air Force Office of Scientific Research. A preliminary report of portions of the present work appears in F. Harbus and H. E. Stanley, Phys. Rev. Lett. **29**, 58 (1972); AIP Conf. Proc. **10**, 884 (1973); and in *Padé Approximants*, edited by P. R. Graves-Morris (Academic, London, 1973), p. 179.

†NSF Predoctoral Fellow.

[1]R. B. Griffiths, Phys. Rev. Lett. **24**, 715 (1970).

[2]I. S. Jacobs and P. E. Lawrence, Phys. Rev. **164**, 66 (1967); W. B. Yelon and R. J. Birgeneau, Phys. Rev. B **5**, 2615 (1972); R. J. Birgeneau and G. Shirane (private communication).

[3]V. A. Schmidt and S. A. Friedberg, Phys. Rev. B **1**, 2250 (1970).

[4]D. P. Landau, B. E. Keen, B. Schneider, and W. P. Wolf, Phys. Rev. B **3**, 2310 (1971); W. P. Wolf, B. Schneider, D. P. Landau, and B. E. Keen, Phys. Rev. B **5**, 4472 (1972).

[5](a) E. H. Graf, D. M. Lee, and J. D. Reppy, Phys. Rev. Lett. **19**, 417 (1967); (b) T. Alvesalo, P. Berglund, S. Islander, G. R. Pickett, and W. Zimmerman, Phys. Rev. Lett. **22**, 1281 (1969); Phys. Rev. A **4**, 2354 (1971); (c) G. Goellner and H. Meyer, Phys. Rev. Lett. **26**, 1534 (1971); (d) G. Ahlers and D. S. Greywall, Phys. Rev. Lett. **29**, 849 (1972). For additional references, see *Cooperative Phenomena near Phase Transitions: A Bibliography with Selected Readings*, edited by H. E. Stanley (MIT Press, Cambridge, Mass., 1973), Part I.

[6]For general reviews, see C. Domb, Adv. Phys. **9**, 149 (1960); M. E. Fisher, Rep. Prog. Phys. **30**, 615 (1967); C. Domb, Adv. Phys. **19**, 339 (1970); H. E. Stanley, *Introduction to Phase Transitions and Critical Phenomena* (Oxford U. P., London, 1971), Chap. 9.

[7]B. Widom, J. Chem. Phys. **43**, 3892 (1965); J. Chem. Phys. **43**, 3898 (1965); C. Domb and D. L. Hunter, Proc. Phys. Soc. Lond. **86**, 1147 (1965); L. P. Kadanoff, Physics (N.Y.) **2**, 263 (1966); R. B. Griffiths, Phys. Rev. **158**, 176 (1967); A. Hankey and H. E. Stanley, Phys. Rev. B **6**, 3515 (1972).

[8]L. P. Kadanoff, in *Proceedings of the Enrico Fermi Summer School*, edited by M. S. Green (Academic, New York, 1971); R. B. Griffiths, Phys. Rev. Lett. **24**, 1479 (1970); G. Paul and H. E. Stanley, Phys. Rev. B **5**, 3715 (1972); S. Milošević and H. E. Stanley, Phys. Rev. B **6**, 1002 (1972).

[9]F. Harbus and H. E. Stanley, following paper, Phys. Rev. B **8**, 1156 (1973).

[10]R. B. Griffiths, in *Critical Phenomena in Alloys, Magnets, and Superconductors*, edited by R. E. Mills, E. Ascher, and R. I. Jaffee (McGraw-Hill, New York, 1971), pp. 377–391.

[11]L. Landau, Phys. Z. Sowjetunion **11**, 26 (1937), reprinted in *Collected Papers of L. D. Landau*, edited by D. ter Haar (Pergamon, New York, 1965), p. 193.

[12]R. B. Griffiths and J. C. Wheeler, Phys. Rev. A **2**, 1047 (1970).

[13]A. Bienenstock, J. Appl. Phys. **37**, 1459 (1966).

[14]A. Bienenstock and J. Lewis, Phys. Rev. **160**, 393 (1967).

[15]J. H. Schelleng and S. A. Friedberg, Phys. Rev. **185**, 728 (1969).

[16]M. E. Fisher, Proc. R. Soc. A **254**, 66 (1960); Proc. R. Soc. A **256**, 502 (1960).

[17]D. C. Rapaport and C. Domb, J. Phys. C **4**, 2684 (1971).

[18]G. A. Baker, Phys. Rev. **124**, 768 (1961).

[19]D. Gaunt and G. A. Baker, Jr., Phys. Rev. B **1**, 1184 (1971).

[20]M. Ferer and M. Wortis, Phys. Rev. B **6**, 3426 (1972).

[21]For work on materials with spin-flop transitions, which are anisotropic Heisenberg systems, with comparatively small anisotropy compared to metamagnets, see, for example, Ref. 15, or V. A. Schmidt and S. A. Friedberg, J. Appl. Phys. **38**, 5319 (1967).

[22]M. Blume, V. J. Emery, and R. B. Griffiths, Phys. Rev. A **4**, 1071 (1971).

[23]This point has been emphasized by E. K. Riedel [Phys. Rev. Lett. **28**, 675 (1972)].

[24]D. M. Saul and M. Wortis, AIP Conf. Proc. **5**, 349 (1972).

[25]J. Oitmaa, J. Phys. C **4**, 2466 (1971); J. Phys. C **5**, 435 (1972).

[26]I. G. Enting and J. Oitmaa, Phys. Lett. A **38**, 107 (1972); J. Oitmaa and I. G. Enting, Phys. Lett. A **36**, 91 (1971); J. Phys. C **5**, 231 (1972); D. C. Rapaport, Phys. Lett. A **37**, 407 (1971); G. Paul and H. E. Stanley, Phys. Rev. B **5**, 2578 (1972); F. Harbus and H. E. Stanley, Phys. Rev. B **7**, 365 (1973); R. Krasnow, F. Harbus, L. L. Liu, and H. E. Stanley, Phys. Rev. B **7**, 370 (1973).

[27]G. Paul and H. E. Stanley, Phys. Rev. B **5**, 3715 (1972), and references contained therein.

[28]D. P. Landau, Phys. Rev. Lett. **28**, 449 (1972).

[29]B. L. Arora and D. P. Landau, AIP Conf. Proc. **10**, 870 (1973).

[30]R. Bidaux, P. Carrara, and B. Vivet, J. Phys. Chem. Solids **28**, 2453 (1967).

[31]A. Hankey, H. E. Stanley, and T. S. Chang, Phys. Rev. Lett. **29**, 278 (1972); see also A. Hankey and H. E. Stanley, Phys. Rev. B **6**, 3515 (1972).

[32]E. K. Riedel, AIP Conf. Proc. **10**, 865 (1973).

[33]T. S. Chang, A. Hankey, and H. E. Stanley, Phys. Rev. B **7**, 4263 (1973); Phys. Rev. B **8**, 346 (1973).

[34]E. K. Riedel and F. J. Wegner, Phys. Rev. Lett. **29**, 349 (1972).

[35]K. G. Wilson, Phys. Rev. B **4**, 3174 (1971); Phys. Rev. B **4**, 3184 (1971).

[36]F. J. Wegner and E. K. Riedel, Phys. Rev. B **7**, 248 (1973), and unpublished work.

[37]P. J. Kortman, Phys. Rev. Lett. **29**, 1449 (1972).

[38]L. Reatto, Phys. Rev. B **5**, 204 (1972).

[39]D. Stauffer, Phys. Rev. B **6**, 1839 (1972).
[40]J. F. Nagle, Phys. Rev. A **2**, 2124 (1970); J. F. Nagle and J. C. Bonner, J. Chem. Phys. **54**, 729 (1971); J. C. Bonner and J. F. Nagle, J. Appl. Phys. **42**, 1280 (1971); W. K. Theumann and J. S. Hoye, J. Chem. Phys. **55**, 4159 (1971); J. S. Hoye, Phys. Rev. B **6**, 4261 (1972); A. Hankey, T. S. Chang, and H. E. Stanley, AIP Conf. Proc. **10**, 889 (1973).
[41]M. Wortis, D. Jasnow, and M. A. Moore, Phys. Rev. **185**, 805 (1969). See also the review article by M. Wortis, in *Phase Transitions and Critical Phenomena*, edited by C. Domb and M. S. Green (Academic, London, to be published), Vol. 3.
[42]F. Englert, Phys. Rev. **129**, 567 (1963).
[43]Thus, in vertex renormalization, one eliminates all so-called "one-insertions" from each skeletal vertex at the expense of replacing bare semi-invariants with renormalized semi-invariants. In bond renormalization, one replaces all "two-insertions" by a single bond which now no longer represents a simple exchange factor J but is rather a more complex correlation factor.
[44]For a study of correlation functions in finite field see D. Gaunt and G. A. Baker, Jr., Phys. Rev. B **1**, 1184 (1971).
[45]F. Harbus and H. E. Stanley, Phys. Rev. Lett. **29**, 58 (1972); the meta model has been recently studied for the special case $H=0$ by A. J. Guttmann, J. Phys. C **5**, 2460 (1972).
[46]M. A. Moore, D. Jasnow, and M. Wortis, Phys. Rev. Lett. **22**, 940 (1969).
[47]See the reviews of Ref. 6 for a general discussion of series-analysis methods; and also D. L. Hunter and G. A. Baker, Phys. Rev. B **7**, 3346 (1973) for a more detailed treatment and critique.
[48]Suppose the series for these models in both finite direct field H and staggered field H_{st} were somehow available. We note that it would be much more difficult to locate by series the critical lines terminating the wings. In the full three-dimensional H-T-H_{st} field space, a ray through the origin at some inclination to the H-T plane is not guaranteed to intersect the wing critical lines, though perhaps such series might be able to respond to singularities on the wings simply by coming close by.
[49]This problem and a bilinear transformation method to deal with it are discussed in M. H. Lee and H. E. Stanley, Phys. Rev. B **4**, 1613 (1971). See also Ref. 51.
[50]M. E. Fisher, Philos. Mag. **7**, 1731 (1962); M. F. Sykes and M. E. Fisher, Physica (Utr.) **28**, 919 (1962); Physica (Utr.) **28**, 939 (1962); M. E. Fisher, *Lectures in Theoretical Physics* (University of Colorado Press, Boulder, Colo., 1965), Vol. VIIc, pp. 1–159.
[51]D. D. Betts, C. J. Elliott and R. V. Ditzian, Can. J. Phys. **49**, 1327 (1971).
[52]We thank Professor R. B. Griffiths for very helpful discussions on this point; see also Ref. 12.

PHYSICAL REVIEW B VOLUME 8, NUMBER 3 1 AUGUST 1973

High-Temperature-Series Study of Models Displaying Tricritical Behavior. II. A Nearest-Neighbor Ising Antiferromagnet with Next-Nearest-Neighbor Ferromagnetic Interactions*

Fredric Harbus† and H. Eugene Stanley
Physics Department, Massachusetts Institute of Technology, Cambridge, Massachusetts 02139
(Received 16 February 1973)

The nnn model is an Ising model with nearest-neighbor antiferromagnetic interactions ($J_1 < 0$) but also next-nearest-neighbor ferromagnetic exchange ($J_2 > 0$). This model is analyzed in external magnetic field using the same techniques as applied to the meta model of Paper I. Again, the staggered susceptibility χ_{st} appears to diverge along the critical line in the H-T plane with a constant exponent $\gamma_{st} = 5/4$, consistent with the universality hypothesis. However, in contrast to the meta model, it is found that the direct susceptibility χ diverges at the tricritical point with an exponent $\bar{\gamma} \simeq 1/4$. Implications of the scaling hypothesis at the tricritical point are discussed and the results for both the meta and nnn models are utilized to obtain the scaling power $\tilde{a}_2$ corresponding to the "weak" direction (in the sense of Griffiths and Wheeler). Included in this discussion is the double-power-law form, predicted to hold within the crossover region by tricritical-point scaling.

I. INTRODUCTION

A next-nearest-neighbor (nnn) spin-$\frac{1}{2}$ Ising model with tricritical behavior was introduced in Eq. (2.4) of the preceding paper[1] (Paper I). The Hamiltonian is

$$\mathcal{H} = -J_1 \sum_{\langle ij \rangle}^{\text{nn}} s_i s_j - J_2 \sum_{[ij]}^{\text{nnn}} s_i s_j - \mu H \sum_i s_i \ . \qquad (1.1)$$

Here $J_1 < 0$ (antiferromagnetic), $J_2 > 0$ (ferromagnetic), and the first and second sums are over nearest-neighbor (nn) and nnn spins, respectively. H is a direct external field, and μ is the magnetic moment per site. The Hamiltonian is considered on the simple-cubic lattice.

We apply the same series-expansion techniques to this model (with $J_1 = -1$, and $J_2 = +\frac{1}{2}$) as were applied to the meta model of Paper I. We therefore do not repeat the discussion of the method of obtaining the series and of the various methods of analysis, but rather go directly to the results. The coefficients of the reduced-susceptibility and stag-